Journal of Applied Electrochemistry **32**: 1229–1233, 2002.

Effect of oxygen flow rate on the structural and electrochemical properties of lithium nickel oxides synthesized by the sol–gel method

K-S. PARK[1], S-H. PARK[1], Y-K. SUN[2], K-S. NAHM[1,*], Y-S. LEE[3] and M. YOSHIO[3]
[1]*School of Chemical Engineering and Technology, College of Engineering, Chonbuk National University, Chonju 561-756, Korea*
[2]*Department of Industrial Chemistry, College of Engineering, Hanyang University, Seoul 133-791, Korea*
[3]*Department of Applied Chemistry, Saga University, 1 Honjo, Saga 840-8502, Japan*
*(*author for correspondence, fax: +82 63 270 2306, e-mail: nahmks@moak.chonbuk.ac.kr)*

Received 30 November 2001; accepted in revised form 17 July 2002

Key words: lithium nickel oxide, oxygen effect, sol–gel method, structural and electrochemical properties

Abstract

The structural and electrochemical properties of $LiNiO_2$ powders were investigated as a function of the oxygen flow rate employed in the preparation of lithium nickel oxide. It was found that oxygen played an important role in the synthesis of highly crystallized $LiNiO_2(R\bar{3}m)$. In the crystallization process of $LiNiO_2$, a deficiency of oxygen in the calcination reactor induced the formation of impurities and cubic rock-salt structure ($Fm3m$) in $LiNiO_2$ powders. For $LiNiO_2$ prepared at higher oxygen flow rates, the electrode delivered high discharge capacities with relatively good retention rates. But very low electrode capacity was obtained from $LiNiO_2$ prepared at lower oxygen flow rates.

1. Introduction

$LiNiO_2$ is a promising cathode material for lithium secondary batteries due to its abundance and environmental advantages over $LiCoO_2$ [1, 2]. In spite of its advantages, $LiNiO_2$ has not been widely used as a cathode material for lithium secondary batteries because it is difficult to synthesize stoichiometric $LiNiO_2$ [3].

Many research groups have employed a variety of synthesis conditions to overcome this barrier and have reported how the synthesis parameters influence the structural and electrochemical properties of the materials produced. Among the parameters, some groups have found that the kind and flow rate of the atmospheric gas during calcination has a serious impact on the crystallization of the synthesized $LiNiO_2$ which significantly influences the electrode performance. Tsutomu [4] and Wang [5] measured the charge–discharge properties of $LiNiO_2$ powders synthesized at 750 °C under the flow of oxygen or air, and reported that the discharge capacity of $LiNiO_2$ synthesized in O_2 was much higher than that in air and that capacity fading occurred rapidly in air, whereas it hardly occurred in the case of the O_2 atmosphere. Meanwhile, Okada et al. [6] observed the appearance of NiO impurity peak from $LiNiO_2$ synthesized in air, but not in O_2 atmosphere. The above work indicates that oxygen may play an important role in the crystallization of $LiNiO_2$ powders, which has serious impact on the electrochemical properties of the electrode. But no reports have clearly showed the effect of oxygen flow rate on the structural and electrochemical properties of $LiNiO_2$.

In this work, we have synthesized $LiNiO_2$ under different oxygen flow rates using a sol–gel method. Structural and electrochemical characterizations were performed for the materials produced. Gas composition was measured during the calcination of $LiNiO_2$ precursors. The role of oxygen during the synthesis of $LiNiO_2$ is discussed, based on the experimental data.

2. Experimental details

$LiNiO_2$ powders were synthesized using a sol–gel method [7]. Stoichiometric amounts of $Li(Li(CH_3COO)\cdot 2H_2O)$ and Ni acetate $(Ni(CH_3COO)_2\cdot 4H_2O)$ salts (cationic ratio of Li:Ni=1:1) were dissolved in DI water. This solution was introduced drop by drop into continuously agitated aqueous adiphic acid solution, which was used as a chelating agent. The molar ratio of adiphic acid to total metal ions was fixed at unity. The mixed solution was evaporated at about 70–80 °C to make a transparent sol. The sol was turned into a viscous transparent gel by further evaporation. The gel precursors were decomposed at 450 °C for 10 h in a box furnace to eliminate organic components. The decomposed powders were postcalcined at 750 °C under oxygen flow for 14 h in a quartz tubular reactor as a

function of oxygen flow rate (100–900 sccm (standard cubic centimetre per minute), and the heating and cooling rates of the powders were 1 °C min^{-1} to prevent the cation mixing in $LiNiO_2$.

After the synthesis, amounts of Li and Ni in the synthesized materials were analysed with an inductively coupled plasma (ICP, Himadachi) to determine the real chemical composition. The oxygen content was determined via mass balance. The structural properties of the synthesized powders were investigated using X-ray powder diffraction (XRD, D/Max-3A, Rigaku) with CuK_α target. Rietveld refinement was carried out using the XRD data to obtain lattice parameters of the synthesized powders.

Quadrapole mass spectroscopy (QMS, HAL2/511, Hiden) was employed to analyse gas composition evolved during the calcination of as-prepared gel precursors (0.5 g) under a flow of 250 ml O_2 min^{-1}. The temperature of the sample was monitored just below the sample holder and raised 5 °C min^{-1} using a PID (proportional integral derivative) controller. The outlet of the reactor was connected to the QMS using a quartz capillary tube (0.5 mm).

The electrochemical characterization was performed using CR2032 coin-type cells. For assembling electrochemical test cells, the cathode was fabricated with accurately weighed active material (20 mg) and conductive binder (13 mg). It was pressed upon 25 mm^2 stainless steel mesh used as the current collector at 300 kg cm^{-2} and dried at 200 °C for 5 h in an oven. This cell consisted of a cathode and a lithium metal anode (Cyprus Foote Mineral Co.) separated by a porous polypropylene film as the separator (Celgard 3401). The electrolyte was 1 M $LiPF_6$–ethylene carbonate (EC)/dimethyl carbonate (DMC) (1:2 by volume). The cell was assembled in an argon-filled dry box and was tested at room temperature. The cell was charged and discharged at a current density of 0.4 mA cm^{-2} ($C/3$) with cut-off voltages of 3.0 to 4.3 V vs Li/Li^+.

3. Results and discussion

The chemically analysed composition of the prepared samples is listed in Table 1 as a function of the oxygen flow rate, together with the calculated composition as well as the XRD data. The chemical analysis shows that the real composition of lithium element for the $LiNiO_2$ synthesized maintains almost 1.0 for all the oxygen flow rates. Although not presented in this paper, SEM photographs showed no difference in the average particle size of the $LiNiO_2$ powders (0.2–0.5 μm).

Figure 1 shows typical XRD spectra for $LiNiO_2$ powders prepared at 750 °C for 14 h as a function of the oxygen flow rate. XRD spectra show that all the samples have a typical $LiNiO_2$ layered structure with a space group $R\bar{3}m$. No impurity related peak is observed from the XRD spectra for the $LiNiO_2$ powders synthesized at O_2 flow rates of 500–900 sccm, but powders prepared at flow rates in the range 100–400 sccm exhibit XRD peaks of LiOH, Li_2CO_3 and Li_2O impurities at $2\theta = 22$, 30 and 33°, respectively. The XRD peak intensities of LiOH, Li_2CO_3 and Li_2O impurities decrease with increasing O_2 flow rate from 100 to 400 sccm. At lower oxygen flow rates, it is considered that carbonaceous residues, originating from the starting materials during the precalcinating process, are not completely removed from the samples and react with lithium to form various impurities during the post calcinating process. All the peaks appearing on the XRD diffractions were identified with the characteristic peaks of $LiNiO_2$ reported in the X-ray powder data file of JCPDS, as well as previously reported work [8].

Shown in the upper inset in Figure 1 is the intensity ratio of (0 0 3) and (1 0 4) peaks obtained from the XRD spectra of Figure 1 as a function of O_2 flow rate. As the O_2 flow rate increases, the intensity ratio of (0 0 3) and (0 1 4) peaks increases up to 500 sccm and maintains almost constant above 500 sccm. According to Morales et al. [9], the (0 0 3) peak is observed from the diffraction of a layered rock-salt structure ($R\bar{3}m$), whereas the (1 0 4) peak appears from both the diffractions of layered and cubic rock-salt structures. In addition, Figure 1 shows that the splitting of the (1 0 1) and (0 0 6) peaks and (1 0 8) and (1 1 0) peaks increase with increasing O_2 flow rate up to 500 sccm and become apparent above 500 sccm. The increase of the splitting of the peaks provides strong evidence for the formation of the $R\bar{3}m$ layered rock-salt phase which has a stable structure and high electrical conductivity [10].

Table 1. Synthetic conditions and structural parameters of $LiNiO_2$ calcined at 750 °C in O_2 flow

$LiNiO_2$ samples	O_2 flow rate /sccm	Bragg ratio (I_{003}/I_{104})	Lattice constants (hexagonal)		Measured Li contents
			a Å	c Å	
A	100	0.6466	2.9814	14.2063	0.99
B	200	0.8852	2.8906	14.2134	0.99
C	300	0.9038	2.8902	14.2207	0.99
D	400	1.1773	2.8832	14.2068	1.00
E	500	1.5991	2.8793	14.2000	1.00
F	600	1.5974	2.8753	14.1933	1.00
G	700	1.5699	2.8757	14.1948	0.99
H	800	1.6155	2.8747	14.1892	1.00
I	900	1.5699	2.8779	14.2000	0.99

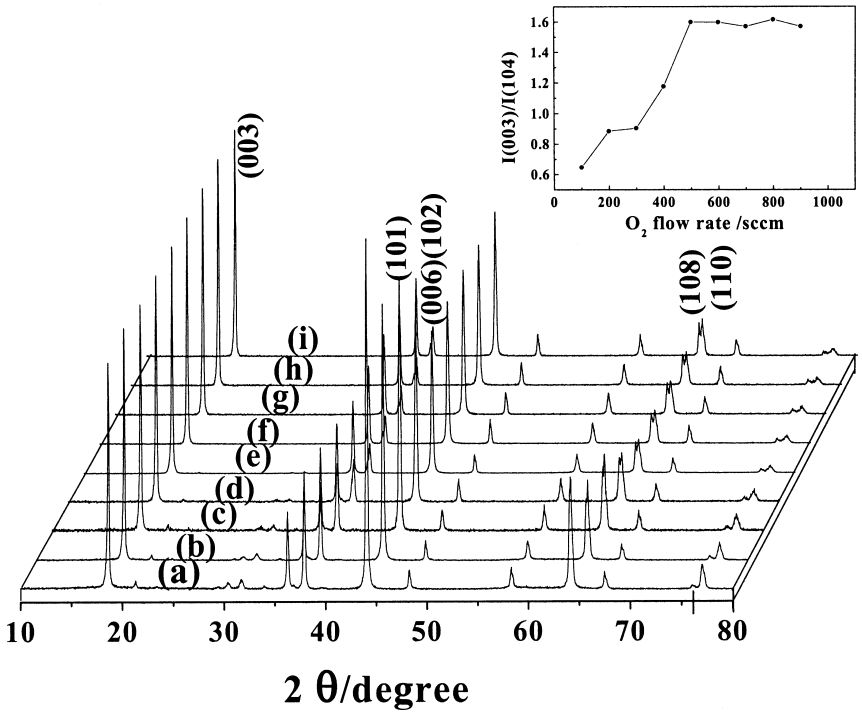

Fig. 1. X-ray diffraction patterns of $LiNiO_2$ at various oxygen flow rates: (a) 100, (b) 200, (c) 300, (d) 400, (e) 500, (f) 600, (g) 700, (h) 800, and (i) 900 sccm. Powders were prepared using sol–gel method at a precalcination temperature of 450 °C in air and calcined again at 750 °C in O_2.

Summarizing the above structural analysis, the best crystallized $LiNiO_2$ powders are synthesized at the O_2 flow rates above 500 sccm.

Figure 2 shows plots of the discharge capacity measured at room temperature against cycle number for samples prepared at 300, 500 and 800 sccm, respectively. The Li/$LiPF_6$–EC/DMC (1:2 by vol.)/$LiNiO_2$ cells were fabricated using sample powders synthesized at various O_2 flow rates ((a) sample C 300 sccm; (b) sample E 500 sccm; (c) sample H 800 sccm). The discharge capacity of the cells increases with increasing the oxygen flow rate. For 300 sccm, the capacity is 56 mAh g^{-1} at the first cycle and dramatically decreases after that cycle to be below 20 mAh g^{-1}. However, unlike sample C, the samples E and H initially deliver high discharge capacities of 163 and 139 mAh g^{-1}, respectively. But the capacitites decrease very slightly with cycle number to 148 and 135 mAh g^{-1} after the 35th cycles with capacity retention rates of 90 and 95%, respectively.

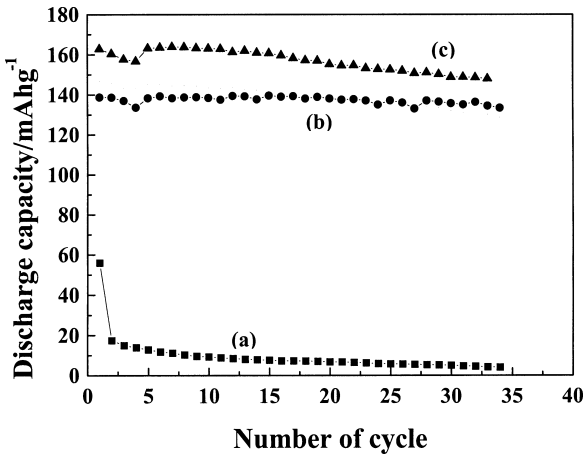

Fig. 2. Plots of specific discharge capacity against number of cycles for the Li /$LiPF_6$–EC/DMC(vol.1:2)/$LiNiO_2$ powders prepared as various O_2 flow rate at 750 °C. Cycling was carried out galvanostatically at constant charge–discharge current density of 0.4 mA cm^{-2} between 3.0–4.3 V at room temperature. Flow rate: (a) 300, (b) 500 and (c) 800 sccm.

The electrochemical behaviour observed above is well explained using the data of the $I(0\,0\,3)/I(1\,0\,4)$ peak intensity ratio and impurities measured as a function of the O_2 flow rate. The electrochemical properties of the cell deteriorate at low O_2 flow rates, which produce the cubic rock-salt phase and impurities in the $LiNiO_2$ powders.

To investigate how the O_2 flow rate influences the synthesis of the crystallized $LiNiO_2$, the composition of the gas mixture produced during the decomposition of the $LiNiO_2$ gel precursor was analysed using a QMS. Figure 3 shows the partial pressures of the gaseous species evolved during the decomposition of the gel precursor as a function of temperature. The moisture in the precursor begins to desorb at above 100 °C. It seems that most of the starting materials used for the synthesis begin to decompose at about 400 °C, which is consistent with TGA and DTA analyses observed previously [7]. The partial pressures of CO_2, H_2O and H_2 gases greatly increase at around 400 °C, whereas the partial pressure of CO is much smaller than that of CO_2. These evolved gases mainly originate from the decomposition of the starting materials and chelating agent. It is interesting to see that the partial pressure of oxygen rapidly decreases from about 400 °C and remains very low in

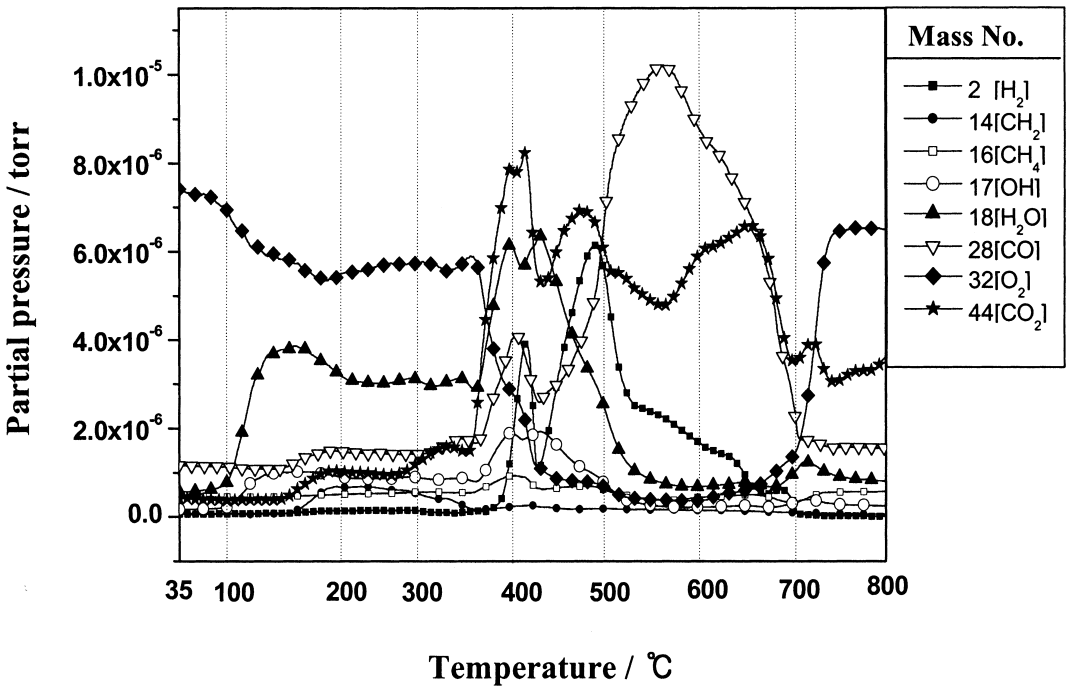

Fig. 3. Plots of partial pressures of gaseous species evolved from $LiNiO_2$ gel precursor during calcination as a function of decomposition temperature.

the temperature range 400–700 °C. At above 700 °C, the partial pressure of oxygen recovers its original value and levels off as the temperature increases further. This indicates that most of the crystallization of $LiNiO_2$ occurs in the temperature range 400–700 °C and the synthetic reaction is terminated at about 700 °C.

The starting materials began to decompose at about 400 °C to produce a gas mixture mainly consisting of CO_2 and H_2O. The evolution of CO_2 and H_2O from the starting materials in the presence of O_2 during the decomposition process is due to the inclusion of acetic ion (CH3COO•) in the starting materials. Meanwhile, it seems that the primary evolution of CO and CO_2 in the crystallization process is due to the oxidation of the deposited carbonaceous residues in the presence of oxygen. The above observation clearly demonstrates that oxygen plays an important role for the synthesis of highly crystallized $LiNiO_2$, as suggested in previous experimental work [4–6].

The structure of $LiNiO_2$ is based on a close-packed network of oxygen anions with ordering of the Li^+ and Ni^{3+} ions on alternating (1 1 1) planes of the cubic rocksalt structure [11]. The precalcination of the gel precursors may produce deposition of carbonaceous residues, originating from the starting materials which contain CH_3 and COO radicals. In the post calcinating process, higher oxygen flow rates may completely remove these carbonaceous residues in the form of CO_2, CO and H_2O by reacting with oxygen. But at lower oxygen flow rates the residues easily reacts with lithium to induce the formation of LiOH, Li_2CO_2 and Li_2O impurities in the $LiNiO_2$. Moreover, $LiNiO_2$ crystallizes in the cubic rock salt structure rather than in the layered rock-salt structure, since 6*c* sites are insufficiently occupied by oxygen. The layered $LiNiO_2$ is easily contaminated with the cubic rock salt domain since the structure of layered $LiNiO_2$ is thermodynamically more unstable than that of cubic $LiNiO_2$ [12]. This was explicitly shown, not only from the $I(0\ 0\ 3)/I(1\ 0\ 4)$ peak ratio, but also from hexagonal lattice parameters *a* and *c* listed in Table 1. As the O_2 flow rate increases, the intensity ratio of the (0 0 3) and (1 0 4) peaks increases up to 500 sccm and remains almost constant when the O_2 flow rate further increases, whereas the parameters *a* and *c* decrease with increasing oxygen flow rate. The increase in *a* and *c* with decrease in O_2 flow rate reflects the increase in the number of Ni^{2+} rather than Ni^{3+} in the lithium nickel oxide. The Ni^{2+} ions partly enter into the lithium layer, which causes cation mixing in the $LiNiO_2$. The increased degree of cation mixing results in the transformation of the layered to cubic $LiNiO_2$ structures, which may interrupt the transfer of the lithium ions, leading to deterioration of the electrode performance during charge and discharge because the cubic structure requires the three-dimensional movement of Li ions [13].

4. Conclusion

It was found that oxygen plays an important role in the synthesis of highly crystallized $LiNiO_2$. The deficiency of oxygen during the crystallization process of $LiNiO_2$ induces the formation of impurities in $LiNiO_2$, as well as the inclusion of cubic rock salt domain in $LiNiO_2$ structure. The deterioration in the $LiNiO_2$ crystallinity

results in a decrease in discharge capacity and poor cyclability.

Acknowledgement

This work was supported by Korea Research Foundation Grant (KRF-2000-E00079).

References

1. C. Delmas, *Mater. Sci. Eng. B, Solid-State Mater. Adv. Technol.* **3** (1989) 97.
2. J.N. Reimers, W. Li, E. Rossen and J.R. Dahn, *in* G.A. Nazri, J.M. Tarascon and M. Armand (Eds), MRS Symposium Proceedings Vol. 293, (MRS, Pittsburg, 1993), p. 3.
3. J.R. Dahn, U. Von Sacken and C.A. Michel, *Solid State Ionics* **44** (1990) 87.
4. T. Ohzuku, A. Ueda and M. Nagayama, *J. Electrochem. Soc.* **140** (1993) 1563.
5. G.X. Wang, S. Zhong, D.H. Bradhurst, S.X. Dou and H.K. Liu, *J. Power Sources* **76** (1998) 141.
6. M. Okada, K-I. Takahashi and T. Mouri, *J. Power Sources* **68** (1997) 545.
7. Y-S. Lee, Y-K. Sun and K-S. Nahm, *Solid State Ionics* **118** (1999) 159.
8. S. Yamada, M. Fujiwara and M. Kanda, *J. Power Sources* **54** (1995) 209.
9. J. Morales, C. Peres-Vicente and J.L. Tirado, *Mat. Res. Bull.* **25** (1990) 623.
10. Y.M. Choi, S.I. Pyun, J.S. Bae and S.I. Moon, *J. Power Sources* **56** (1995) 25.
11. C. Delmas and M.S. Dresselhaus (Eds), 'Intercalation in Layered Materials', *NATO. ASI. B*, **148** (1986) 155.
12. T. Ohzuku, A. Ueda, M. Nagayama, Y. Iwakoshi and H. Komori, *Electrochimica Acta* **38**(9) (1993) 1159.
13. K. Kubo, M. Fujiwara, S. Yamada, S. Arai and M. Kanda, *J. Power Sources* **68** (1997) 553.